BIOCHEMISTRY
including biophysical chemistry & molecular biology
Article

Biochemistry **2010,** *49,* 5213–5224 5213
DOI: 10.1021/bi1003734

Conformation of Dimeric Apolipoprotein A-I Milano on Recombinant Lipoprotein Particles†

Shaila Bhat,‡ Mary G. Sorci-Thomas,‡,§ Laura Calabresi,∥ Michael P. Samuel,§ and Michael J. Thomas*,§

§*Departments of Biochemistry, and* ‡*Pathology, Center for Lipid Science, Wake Forest University Health Sciences, Medical Center Boulevard, Winston-Salem, North Carolina 27157, and* ∥*Center Grossi Paoletti, Department of Pharmacological Sciences, Università degli Studi di Milano, Via Balzaretti 9, 20133 Milano, Italy*

Received March 10, 2010; Revised Manuscript Received May 11, 2010

ABSTRACT: Apolipoprotein A-I Milano (apoA-I_{Milano}) is a naturally occurring human mutation of wild-type apolipoprotein A-I (apoA-I_{WT}) having cystine substituted for $arginine_{173}$. Two molecules of apo-I_{WT} form disks with phospholipid having a defined relationship between the apoA-I_{WT} molecules. ApoA-I_{Milano} forms cystine homodimers that would not allow the protein to adopt the conformation reported for apoA-I_{WT}. The conformational constraints for dimeric apoA-I_{Milano} recombinant high-density lipoprotein (rHDL) disks made with phospholipid were deduced from a combination of chemical cross-linking and mass spectrometry. Lysine-selective homobifunctional cross-linkers were reacted with homogeneous rHDL having diameters of 78 and 125 Å. After reduction, cross-linked apoA-I_{Milano} was separated from monomeric apoprotein by gel electrophoresis and then subjected to in-gel trypsin digest. Cross-linked peptides were confirmed by MS/MS sequencing. The cross-links provided distance constraints that were used to refine models of lipid-bound dimeric apoA-I_{Milano}. These studies suggest that a single dimeric apoA-I_{Milano} on 78 Å diameter rHDL girdles the edge of a phospholipid disk assuming a "belt" conformation similar to the "belt" region of apoA-I_{WT} on rHDL. However, the C-terminal end of dimeric apoA-I_{Milano} wraps around the periphery of the particle to shield the fatty acid chains from water rather than folding back onto the "belt" as does apoA-I_{WT}. The two apoA-I_{Milano} dimers on a 125 Å diameter rHDL do not encircle the periphery of a phospholipid disk but appear to reside on the surface of a laminar micelle.

HDL plays a central role in a process called reverse cholesterol transport (*1*, *2*) where apolipoprotein A-I (apoA-I)[1], the principal protein associated with HDL, collects and organizes phospholipid and cholesterol that have been removed from extrahepatic cells. There is a large body of evidence demonstrating an inverse correlation between plasma HDL and the risk of developing atherosclerosis (*3*−*6*). However, all carriers of an apoA-I mutation in which cysteine is substituted for arginine at 173, named apoA-I Milano (apoA-I_{Milano}), have low levels of plasma HDL cholesterol and apoA-I. The low levels of plasma HDL would suggest that carriers of the Milano mutation would be at high risk for atherosclerosis, but the contrary was reported (*7*, *8*). Clinical trials in which repeated intravenous infusions of lipid-complexed apoA-I_{Milano} were administered to patients with coronary disease showed a reduction in the volume of atherosclerotic lesions (*9*, *10*), while several animal studies have demonstrated that intravenous injection of apoA-I_{Milano} regressed atherosclerosis in apoE knockout mice (*11*−*14*), rabbits (*15*−*17*), and pigs (*18*). Several animal studies employing targeted replacement of apoA-I with apoA-I_{Milano} have supported the hypothesis that apoA-I_{Milano} was more atheroprotective (*19*) than wild-type apoA-I (apoA-I_{WT}) while other studies have suggested that apoA-I_{Milano} was no more effective than apoA-I_{WT} (*20*, *21*).

It is not known to what extent the apoA-I_{Milano} mutation at residue 173 alters the lipid-bound conformation, but molecular modeling indicates that monomeric apoA-I_{Milano} on rHDL disks assumes a "belt" configuration (*22*) similar to that reported for apoA-I_{WT} (*23*). Because apoA-I_{Milano} is present in plasma as a homodimer or as a herterodimer with apoA-II, it has been assumed that the Cys_{173}−Cys_{173} disulfide linkage between helix 7 of one monomer and helix 7 of the second apoA-I_{Milano} molecule in the homodimer forces the two apoA-I monomers on rHDL to assume a conformation that is different (*24*) from that suggested for apoA-I_{WT} (*23*, *25*−*31*). Therefore, there would be no overlap of the helix 5 to helix 5 region that is a major feature of the lipid-bound conformation (*32*−*36*).

Considerable agreement exits among the various published models of apoA-I_{WT} on POPC rHDL, suggesting that repeats 2 through 8, called the central region, of lipid-bound apoA-I_{WT} assumes an antiparallel orientation with a helix 5 to helix 5

†These studies were supported by grants from the National Institutes of Health (NIH) HL-49373 and HL-64163 (M.G.S.-T.) and from the American Heart Association (M.J.T.).

*To whom correspondence should be addressed. Telephone: (336) 716-2313. Fax: (336) 716-6279. E-mail: mthomas@wfubmc.edu.

[1]Abbreviations: 2F, peptide Ac-DWLKAFYDKVAEKLKEAF-NH_2; 4F, peptide Ac-DWFKAFYDKVAEKFKEAF-NH_2; apoA-I, apolipoprotein A-I; apoA-I_{Milano}, mutant apolipoprotein A-I having R173C; βME, β-mercaptoethanol; BS^3, bis(sulfosuccinimidyl) suberate; $BS(PEG)_5$, bis(*N*-succinimidyl)pentaethylene glycol ester; CCL, lysine-selective chemical cross-linker; CCL/MS, chemical cross-linking combined with mass spectrometry; DMPC, 1,2-dimyristoylphosphatidylcholine; DOPC, dioleoylphosphatidylcholine; DSG, disuccinimidyl glutarate; DSP, dithiobis(succinimidyl propionate); DTT, dithiothreitol; EGS, ethylene glycol bis(succinimidyl succinate); HDL, high-density lipoprotein; LC, liquid chromatography; MS/MS, tandem mass spectrometry; nHDL, nascent HDL; POPC, 1-palmitoyl-2-oleoylphosphatidylcholine; QTOF-MS, quadrupole time-of-flight mass spectrometer; rHDL, recombinant HDL; SANS, small-angle neutron scattering; SAXS, small-angle X-ray scattering; apoA-I_{WT}, wild-type apoA-I.

Published on Web 06/04/2010

registry; e.g., central amphipathic helices on each apoA-I_{WT} monomer are next to one another (*22*, *23*, *25*−*29*, *32*, *36*−*42*). The results of Wu et al. (*29*) and Martin et al. (*43*) suggest that the two apoA-I_{WT} chains do not wrap around the phospholipid disk forming smooth loop but imply that there is additional protein structure important for LCAT activation and reverse cholesterol transport. Both Wu et al. (*26*, *29*) and Bhat et al. (*23*, *25*) suggest that the C-terminal end is somewhat folded back onto the central region or "belt" as proposed by Bhat et al. (*23*, *25*). However, the principal debate or differences between the models center on ascertaining the conformation assumed by the N- and C-terminal ends.

All models to date suggest that the N- and C-terminal ends are close to one another. However, Wu et al. (*29*) suggest that the N-terminal end is relatively disordered while Bhat et al. (*23*, *25*) have suggested that both the N- and C-termini are relatively ordered and interact with the central part of the apoA-I_{WT} molecule. Since the results from chemical cross-linking/mass spectrometry (CCL/MS) yield only a time-averaged conformation, it appears that the N-terminal ends of apoA-I_{WT} spend a significant amount of time close to the "belt" but does not rule out appreciable mobility for the N-terminus that would allow this region to extend into solution and to possibly overlap with its own C-terminus. Importantly, it should be noted that CCL is conducted at low cross-linker to protein ratios; thus only one or two cross-links per apoA-I molecule are formed. This ensures that the formation of cross-links does induce artifactual change to the native conformation of the protein. Therefore, CCL/MS provides a snapshot of the protein conformation at the time the covalent bonds are formed and provides a powerful method for determining three-dimensional experimental coordinates of protein conformation in solution.

In the present report we show our findings regarding the conformation of disulfide-coupled apoA-I_{Milano} dimers on rHDL made from POPC. Dimeric apoA-I_{Milano} complexed with POPC yielded rHDL with diameters of 78 and 125 Å that were analyzed using CCL/MS techniques. In answer to the question "could the unique structure of apoA-I_{Milano} affect the biochemical properties of rHDL", we find that the conformation for apoA-I_{Milano} on rHDL had many similarities to the conformation of apoA-I_{WT} on rHDL, particularly in the "belt" region, but that there were also significant differences in the folding of the N- and C-terminal ends or "buckles" when bound to lipid.

EXPERIMENTAL PROCEDURES

Materials. Bis(sulfosuccinimidyl) suberate (BS^3), dithiobis-(succinimidyl propionate) (DSP), disuccinimidyl glutarate (DSG), bis(*N*-succinimidyl)pentaethylene glycol ester ($BS(PEG)_5$), and ethylene glycol bis(succinimidyl succinate) (EGS) were from ThermoFisher. POPC and Me_2SO were from Sigma-Aldrich. Sequencing grade modified trypsin and restriction enzymes were from Promega. RapiGest SF was obtained from Waters Inc. Formic acid was from Sigma-Aldrich. Sodium deoxycholate, potassium chloride, optima grade methanol, chloroform, acetonitrile, and glacial acetic acid were from Fisher Scientific. Mark 12 molecular weight standards and Simply Blue Safestain were from Invitrogen. Ultrafree-15 centrifugal and Biomax 10K membranes were from Millipore Corp.

Preparation and Purification of rHDL from POPC and Human ApoA-I_{Milano}. Dimeric human apoA-I_{Milano} was purified from the plasma of human carriers in the laboratory of Dr. Laura Calabresi (*24*). ApoA-I_{Milano} purity was analyzed by both 12% SDS−PAGE and mass spectrometry before use. Preparations of all rHDL were carried out as previously described (*44*) using the cholate dialysis method (*45*). Briefly, all preparations employed sodium cholate:POPC at a molar ratio of 1:1 with about 5 mg of dimeric apoA-I_{Milano}. The 125 Å diameter particles containing two dimers of apoA-I_{Milano} were prepared from a starting mixture of 120:1 POPC:dimeric apoA-I_{Milano}, while rHDL particles having a diameter of 78 Å containing one dimer of apoA-I_{Milano} were prepared from a starting molar ratio of 40:1 POPC:dimeric apoA-I_{Milano}. POPC rHDL were prepared after reducing dimeric apoA-I_{Milano} to monomeric apoA-I_{Milano} with 100 mM DTT that was added 30 min before mixing with POPC. The molar ratios of POPC:monomeric apoA-I_{Milano} were 120:1 and 40:1, respectively, like those employed to prepare rHDL particles from wild-type apoA-I (*23*, *25*). After removal of sodium cholate by extensive dialysis the particles were purified by FPLC (*44*).

Gradient Gel Electrophoresis (*4*−*30%*). The diameters of POPC containing rHDL were determined using nondenaturing 4−30% gradient PAGE as previously described (*42*, *46*). Gels were run at 2800 V/h to ensure that the particles had migrated to equilibrium, then fixed, and stained (*47*). rHDL particle size was determined by comparison to protein standards of known Stokes' diameter (*46*) using a standard mixture from GE Healthcare catalogue no. 17-0445-01.

Cross-Linking of rHDL. Cross-linkers were dissolved in dry Me_2SO to a final concentration of 5 μg/μL and used within 5 min of preparation. The cross-linkers were added at molar ratios of 2:1 and 10:1 with a final rHDL apoA-I particle concentration of 0.4 μg/μL in 10 mM sodium phosphate, pH 7.4 (*25*). After the cross-linker was added, the reaction was incubated for 5 min at 37 °C and then quenched by adding 1 M Tris, pH 7.4, giving a final concentration of 50 mM Tris. Samples were dialyzed against 10 mM ammonium bicarbonate, pH 7.4, at 4 °C to remove excess cross-linker. All samples were stored at −20 °C until processed.

SDS−PAGE and In-Gel Trypsin Digest. Products from CCL apoA-I_{Milano} rHDL were separated on 12% SDS−PAGE under both nonreducing (*23*) and reducing conditions. Comparison of product migration between reducing and nonreducing conditions allowed the distinction between "true" chemical cross-links and disulfide-bonded monomers. Protein bands were excised from the gel, minced, and repeatedly dehydrated with acetonitrile. The gel pieces were rehydrated with a cold, freshly prepared solution containing 20 ng/μL trypsin in 10 mM ammonium bicarbonate, pH 7.8, 0.1% (w/v) RapiGest SF, and 1 mM $CaCl_2$, as previously described (*23*, *25*). The final trypsin to apoA-I_{Milano} mass ratio was 1:20. Samples were incubated on ice for 10 min to minimize autolysis while trypsin diffuses into the gel. Then the samples were digested for 18 h at 37 °C.

Peptide Isolation and ES/Q-TOF Mass Spectrometry. Following digestion the aqueous solution was removed, and the gel pieces were covered with 200 μL of extraction solvent (acetonitrile/formic acid/water, 50:5:45 v/v/v). After the slices were incubated for 10 min, the solvent was transferred to a fresh tube. The extraction process was repeated, and the combined aliquots were acidified to an HCl:apoA-I ratio of 1:10 (v/v) using 500 mM HCl. After the acidified solution was incubated for 35 min at 37 °C, precipitate was removed by centrifuging for 10 min at 13000 rpm. The supernatant was transferred to a fresh tube before processing for mass spectrometry.

To identify candidate cross-linked peptides for MS/MS sequencing, survey scans were performed on each peptide mixture

using a Waters Q-TOF API-US mass spectrometer equipped with a Waters CapLC. Acquisition was controlled by MassLynx 4.0 software (*23*, *25*). Peptides were loaded onto a PLRP-S trapping column, 0.5 mm diameter × 2.0 mm length, packed with 3 μm diameter particles having a pore diameter of 100 Å. Peptides were loaded onto the column in water/acetonitrile/formic acid (97:3:0.2) at 500 nL/min and then separated by gradient elution: solvent A (25 mM formic acid in 97% water and 3% acetonitrile) and solvent B (25 mM formic acid in 3% water and 97% acetonitrile). The gradient profile was as follows: 2% solvent B for 3 min, then a linear increase to 40% B at 90 min, and then to 80% B in 5 min. At 95 min the solvent composition was ramped to 2% B over 5 min and then equilibrated with 2% B for 30 min before the next injection. Peptides were eluted at 470 nL/min. Positive ion electrospray survey scans were recorded in the continuum mode using a scan window from m/z 300 to 1500 with an accumulation time of 2 s. The source temperature was 80 °C, and the cone and capillary voltages were 45 V and 3.5 kV, respectively. The experimental m/z was corrected for the +2 charge state using apoA-I tryptic fragment 7, m/z = 806.8969, and for the +1 charge state using apoA-I tryptic fragment 12, m/z = 831.4365. The survey ion scan was deconvoluted to give a list of +1 charge states that eluted from the column. This experimental list was sorted against a list of all possible lysine-to-lysine cross-links for the particular chemical cross-linker used in an experiment. All experimental ions within m/z ±0.051 of the theoretical ions were sequenced. Product ion MS/MS spectra were acquired in the continuum mode from m/z 50 to 1800 using a data-directed charge-state-selective collision energy and an accumulation time of 2s. Sequence analysis of the MS/MS spectra was performed with a fragment ion tolerance of m/z ±0.05.

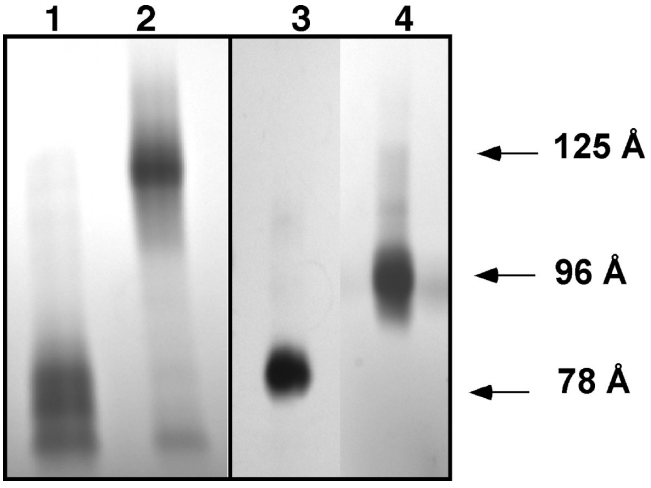

FIGURE 1: Nondenaturing 4−30% gradient gel electrophoresis of recombinant HDL (rHDL) containing POPC and apoA-I_{Milano}. Lane 1, purified 78 Å diameter rHDL prepared using dimeric apoA-I_{Milano}, as described in Experimental Procedures and containing a total of 76 POPC to 1 apoA-I_{Milano} dimer per particle; lane 2, purified 125 Å diameter rHDL containing a total of 209 POPC, with two apoA-I_{Milano} dimers per particle; lane 3, purified 80 Å rHDL prepared with "reduced" apoA-I_{Milano} monomers and having a total of 55 POPC to two apoA-I monomers; lane 4, purified 96 Å rHDL prepared with "reduced" apoA-I_{Milano} monomers and having a total of 150 POPC to two apoA-I monomers. All rHDL preparations were purified by FPLC. Approximately 6 μg of protein was loaded into each lane. High molecular weight markers from GE Healthcare (17-0445-01) were used to calculate each rHDL diameter: 170 Å, ferritin; 124 Å, catalase; 98 Å, lactate dehydrogenase; 82 Å, albumin.

Molecular Modeling of Lipid-Bound ApoA-I_{Milano}. The molecular modeling for apoA-I_{WT} has been described in previous

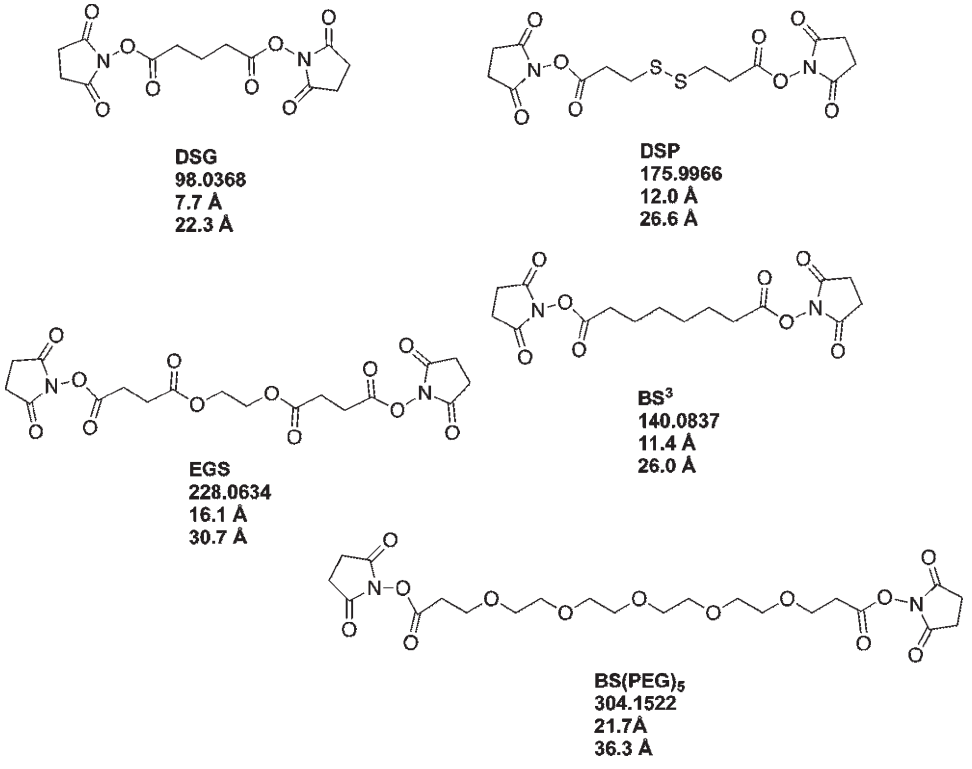

FIGURE 2: Chemical structure of the lysine-reactive homobifunctional cross-linkers used in these studies. Shown are the chemical structure, spacer arm molecular weight, spacer arm length (Å), and C_α−cross-linker−C_α distance (Å) for each cross-linker used in these studies. Each cross-linker contains an amine-reactive NHS ester that can react with any of the 21 lysines found in a single molecule of apoA-I. The cross-linkers and their abbreviations are as follows: DSG, disuccinimidyl glutarate; DSP, dithiobis(succinimidyl propionate); BS^3, bis(sulfosuccinimidyl) suberate; EGS, ethylene glycol bis(succinimidyl succinate); and $BS(PEG)_5$, bis(*N*-succinimidyl)pentaethylene glycol ester. Note: only the cross-linker DSP contains a disulfide linkage that can be "reduced" by treatment with dithiothreitol or β-mercaptoethanol.

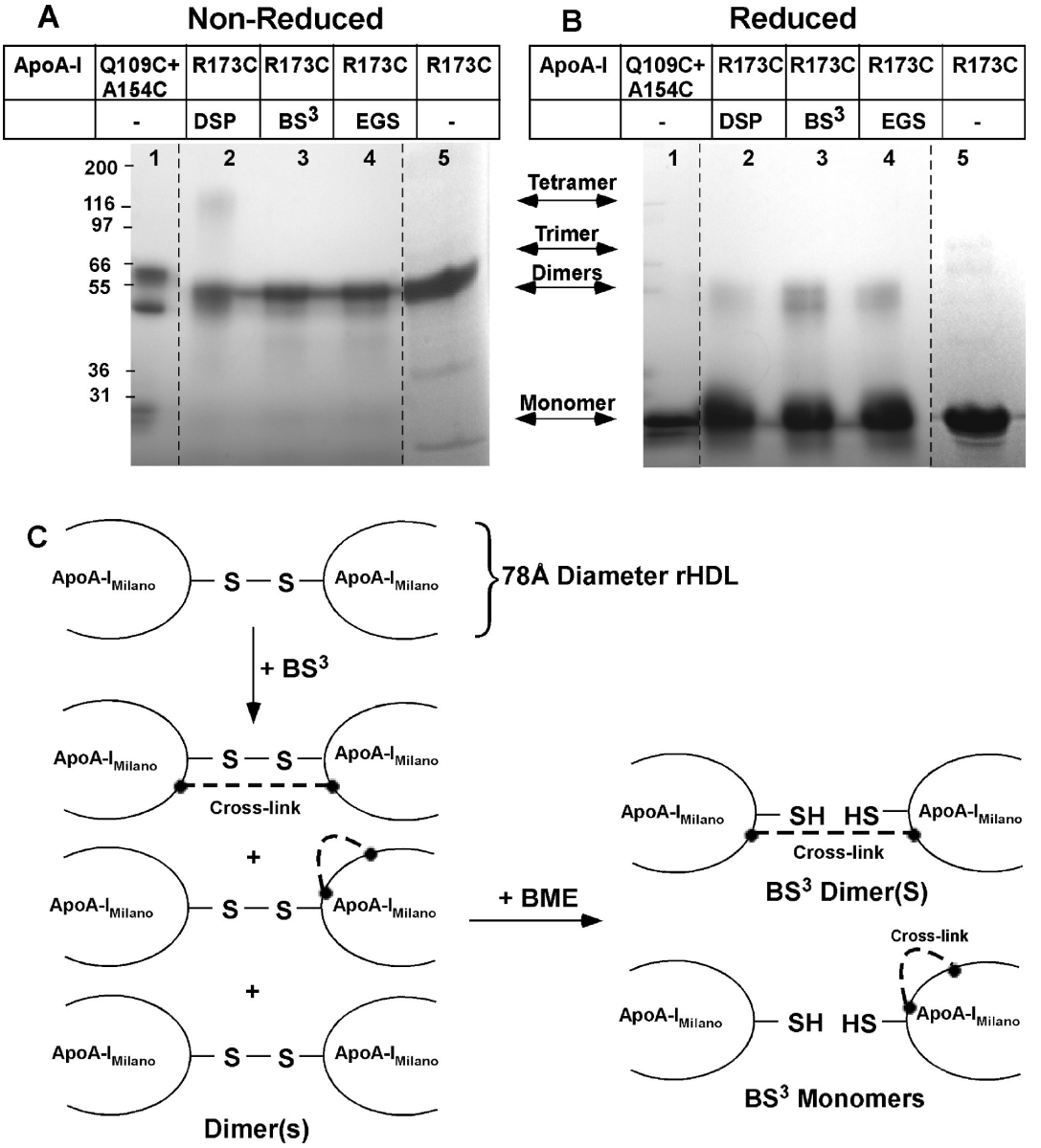

FIGURE 3: 4−30% gradient SDS−PAGE analysis of cross-linked 78 Å diameter POPC:apoA-I_{Milano} rHDL. Panel A shows migration under nonreducing conditions. Panel B shows migration under reducing conditions after treatment with βME. Lane 1 shows the positional specific migration of a mixture of Q109C and A154C apoA-I homodimers (*25*). Lanes 2−4 show 78 Å diameter POPC:apoA-I_{Milano} treated with DSP (lane 2), BS^3 (lane 3), and EGS (lane 4). Lane 5 contains un-cross-linked apoA-I_{Milano}. Mark 12 (Invitrogen) molecular weight markers were used. All samples were treated with a molar ratio of 10:1 cross-linker to apoA-I for 5 min at 37 °C, as described under Experimental Procedures. The dashed lines indicate that lanes have been added or removed. A lane between lanes 1 and 2 was removed. Lane 5 from another SDS−PAGE analysis was added to the figure to show the migration of dimeric apoA-I_{Milano}. Panel C illustrates the pattern of cross-linking for 78 Å diameter rHDL particles that carry a single disulfide-linked dimer of apoA-I_{Milano}. Dashed lines depict chemical cross-links which can be intramolecular or intermolecular. The labels monomer, dimer, trimer, and tetramer indicate where the apoA-I_{Milano} or multimers having 2, 3, or 4 apoA-I_{Milano} would migrate on the gel.

publications (*23*, *25*) using the X-ray crystal coordinates for lipid-free Δ43-apoA-I (*34*) that were joined with the first 43 amino acids of the N-terminal end. Structural studies of unmodified lipid-free apoA-I were used to guide the 1−43 conformation (*48*−*52*). Using a similar approach to our elucidation of the lipid-bound conformation of apoA-I_{WT}, three pieces of information were used to model the spatial relationship of the two molecules of apoA-I_{Milano} on the POPC-containing particles. The first step was to orient the two molecules to accommodate the disulfide cross-link between cysteines at position 173 on each monomer. Then the cross-linked positions on the individual apoA-I molecules were oriented to their correct distances. To do this, we used the maximum distance of C_α-lysine−(cross-linker)−C_α-lysine calculated for each of the cross-linkers: 26.0, 26.6, 30.7, and 36.3 Å for BS^3, DSP, EGS, and $BS(PEG)_5$, respectively. Third, apoA-I was bent only at the proline or glycine−glycine sites between the amphipathic segments of apoA-I. Tools available in Swiss-PdbViewer OSX v4.0.1 (http://www.expasy.org/spdbv/) were used to optimize the conformations while PDB files were manipulated using PyMOL version 1.2r3 (http:/www.pymol.org). Swiss-PdbViewer and PyMOL, along with visual molecular dynamics (VMD) for Mac OSX version 1.8.7 (*53*), were used to generate the molecular figures shown in this report.

RESULTS

Characterization and Cross-Linking of 78 and 125 Å rHDL Containing ApoA-I_{Milano}. To probe the effect that the

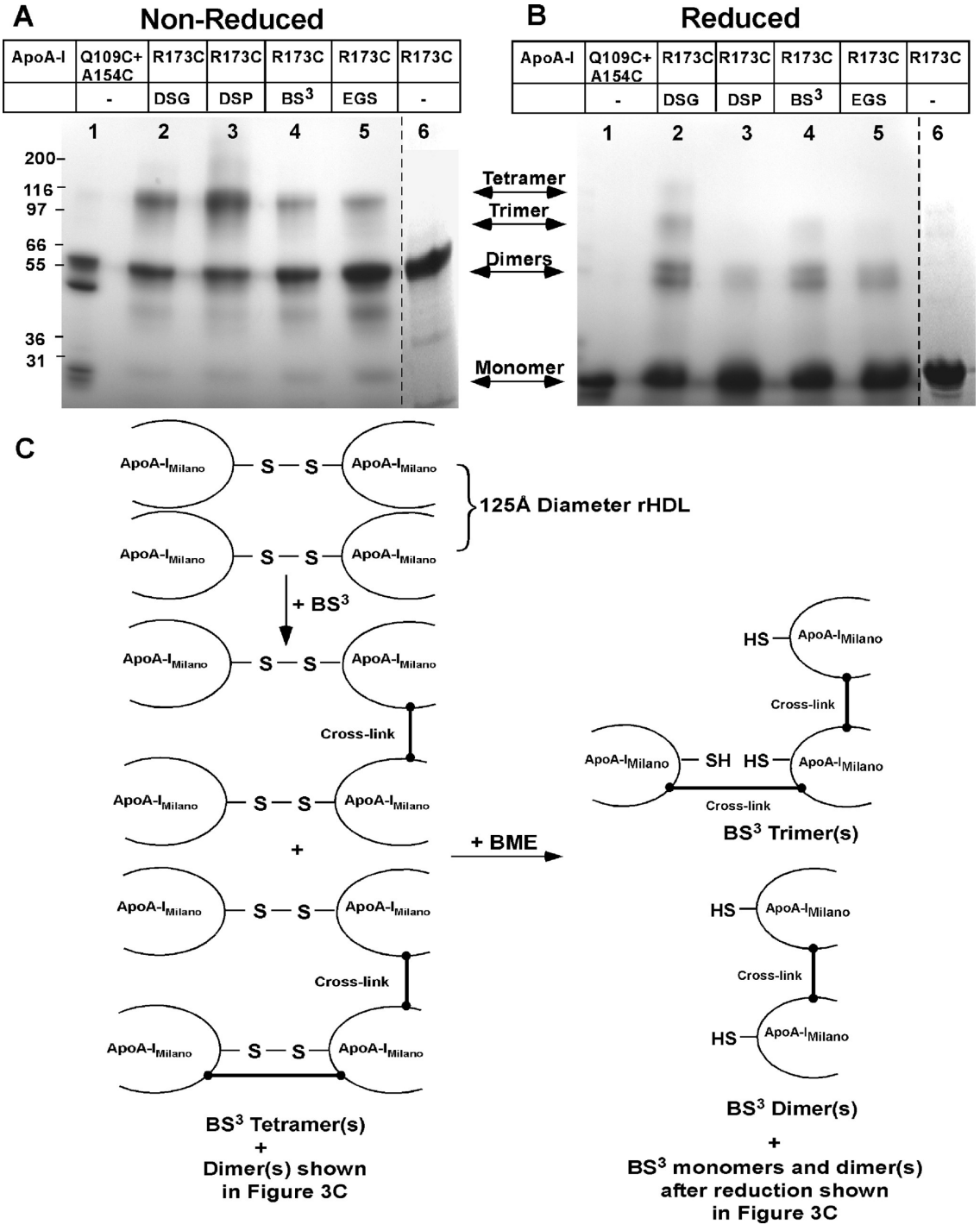

FIGURE 4: 4−30% gradient SDS−PAGE analysis of cross-linked 125 Å diameter POPC:apoA-I_{Milano} rHDL. Panel A shows migration under nonreducing conditions. Panel B shows migration under reducing conditions after treatment with βME. Lane 1 shows the positional specific migration of a mixture of Q109C and A154C apoA-I homodimers (*25*). Lanes 2−5 show 125 Å diameter POPC:apoA-I_{Milano} treated with DSG (lane 2), DSP (lane 3), BS^3 (lane 4), and EGS (lane 5). Lane 6 contains un-cross-linked apoA-I_{Milano}. All samples were treated with 10:1 cross-linker to protein for 5 min at 37 °C, as described under Experimental Procedures. The dashed lines indicate that lanes have been added or removed. Lane 6 from another SDS−PAGE analysis was added to the figure to show the migration of dimeric apoA-I_{Milano}. Panel C illustrates the pattern of cross-linking for 125 Å diameter rHDL particles containing two disulfide-linked dimers of apoA-I_{Milano}. Note that in the absence of interparticle cross-linking only the 125 Å diameter rHDL particle can generate a product that is composed of 4 cross-linked apoA-I_{Milano}, a tetramer.

R173C mutation would impose on the formation of recombinant HDL, we made POPC containing rHDL with both dimer apoA-I_{Milano} and monomeric apoA-I_{Milano}. Interestingly, when the rHDL was made with increasing amounts of POPC and intact dimeric apoA-I_{Milano}, particles with two different diameters were obtained. The first was a 78 Å diameter particle containing a total of 76 molecules of POPC and one dimer of apoA-I_{Milano} per particle, while the other was a 125 Å diameter rHDL containing approximately 209 molecules of POPC and two dimers of apoA-I_{Milano} per particle (*44*), as shown in the nondenaturing 4−30% GGE in Figure 1, lanes 1 and 2. However, when dimeric apoA-I_{Milano} was reduced before being added to POPC, 80 and 96 Å rHDL were formed, as shown in Figure 1, lanes 3 and 4. The 80 and 96 Å rHDL particles contain a total of 55 and 150 molecules

Table 1: Cross-Links Identified from 78 Å Diameter rHDL

sequenced m/z		peptide m/z MH^+ [a] exptl	peptide m/z MH^+ [a] theoretical	m/z error	cross-linker	ID	cross-linked positions	peptides[a]
684.68	+3[b]	2052.0244	2052.0146	0.0098	DSP	T_{2-4}	12−23	11−27
854.86[c]	+2	1708.7122	1708.7596	−0.0474	DSP/BS^3	T_{11-13}	88−94	84−96
954.79[c]	+3	2862.3544	2862.3647	−0.0103	DSP/BS^3	$T_{1\alpha}/T_{2-3}$	1−12	1−10, 11−23
1170.06[c]	+2	2339.1122	2339.1198	−0.0076	DSP/BS^3	T_{20-22}	133−140	132−149
913.14	+3	2737.4373	2737.4365	0.0008	BS^3	T_{5-6}/T_{35-36}	40−239	28−45, 239−243
872.80	+3	2616.4028	2616.4037	−0.0009	BS^3	T_{6-8}	45−59	41−61
783.08	+3	2347.2388	2347.2509	−0.0121	BS^3	T_{31-32}	206−208	196−215
820.10	+3	2458.3232	2458.3303	−0.0071	BS^3	T_{13-14}/T_{17-18}	96−118	95−106, 117−123
760.89	+4	3040.5620	3040.5547	0.0073	BS^3	T_{13-14}/T_{13-14}	96−96	95−106, 95−106
793.66	+4	3171.6382	3171.6636	−0.0254	BS^3	T_{7-8}/T_{20-21}	59−133	46−61, 132−140
777.76	+5	3884.9016	3884.9288	−0.0272	S−S	T_{26-27}/T_{26-27}	173−173	161−177, 161−177

[a]Starting and ending amino acids for each peptide component are given. [b]The charge on the sequenced ion is shown in the second column. [c]Ions from both cross-linkers were sequenced, but only the m/z for the DSP cross-linked ions are shown.

Table 2: Cross-Links Identified from 125 Å Diameter rHDL

sequenced m/z		peptide m/z MH^+ [a] exptl	peptide m/z MH^+ [a] theoretical	m/z error	cross-linker	ID	cross-linked positions	peptides[a]
836.91[b]	+2[c]	1672.8584	1672.8468	0.0116	BS^3/EGS	T_{11-13}	88−94	84−96
731.39	+3	2192.1384	2192.1565	−0.0181	BS^3	T_{13-14}/T_{35-36}	96−239	95−106, 239−243
718.02	+3	2152.0525	2152.0713	−0.0188	BS^3	T_{15-16}/T_{35-36}	107−239	107−116, 239−243
768.3[b]	+3	2303.1929	2303.2069	−0.0140	BS^3/EGS/$BS(PEG)_5$	T_{20-22}	133−140	132−149
820.10	+3	2458.3291	2458.3303	−0.0012	BS^3	T_{13-14}/T_{17-18}	96−118	95−106, 117−123
913.14[b]	+3	2737.4216	2737.4365	−0.0149	BS^3/DSG	T_{5-6}/T_{35-36}	40−239	28−45, 239−243
812.41	+3	2435.2029	2435.2305	−0.0276	EGS	T_{31-32}	206−208	196−215
1052.56	+2	2104.0852	2104.0813	0.0039	EGS	T_{2-4}	12−23	11−27
1066.04	+2	2131.0386	2131.0196	0.0190	$BS(PEG)_5$	$T_{1\alpha}/T_{35-36}$	α-239	1−10, 239−243
799.72	+3	2397.1863	2397.1939	−0.0076	$BS(PEG)_5$	$T_{1\alpha}/T_{17-18}$	α-118	1−10, 117−123
970.14	+3	2908.4302	2908.3887	0.0415	$BS(PEG)_5$	$T_{1\alpha}/T_{14-15}$	α-106	1−10, 97−107
972.01	+4	3884.8782	3884.9288	−0.0506	S−S	T_{26-27}/T_{26-27}	173−173	161−177, 161−177

[a]Starting and ending amino acids for each peptide component are given. [b]Ions from both cross-linkers were sequenced, but only the m/z for BS^3 cross-linked ions are shown. [c]The charge on the sequenced ion is shown in the second column.

of POPC per particle, respectively, and both contain two monomers of apoA-I_{Milano} per particle. These data strongly suggest a conformational restriction imposed by the helix 7 to helix 7 cystine linkage present in the apoA-I_{Milano} dimer appears to cause a significant change in the ability of the apoprotein to stably accommodate phospholipids.

Purified rHDL containing dimeric apoA-I_{Milano} were treated with the homobifunctional, amine-specific cross-linkers BS^3, DSG, DSP, EGS, or $BS(PEG)_5$. The chemical structures of these cross-linkers are shown in Figure 2 along with their carbonyl to carbonyl mass, arm length in angstroms, and the C_α to C_α length in angstroms that includes the lengths of two lysine side chains. Each of these cross-linkers was used at a mole ratio of 10:1 per rHDL apoA-I_{Milano}. Because the size and composition of rHDL containing monomeric apoA-I_{Milano} were the same as that found for rHDL made with apoA-I_{WT} (*25*), further studies using these particles were not conducted.

Cross-linked protein from 78 Å diameter POPC rHDL particles carrying dimeric apoA-I_{Milano} was separated by 4−30% nonreducing gradient SDS−PAGE as shown in Figure 3A or under reducing conditions as shown in Figure 3B. Each gel shows the product distribution following treatment with DSP, lanes 2; BS^3, lanes 3; EGS, lanes 4; and rHDL containing unmodified apoA-I_{Milano}, lanes 5. A mixture of the homodimers, Q109C apoA-I and A154C apoA-I, is shown in lanes 1 to indicate the extremes of aberrant molecular size migration induced by the alternative conformations of apoA-I dimers, as described previously (*25*).

As mentioned before, apoA-I_{Milano} exists as a cysteine disulfide bridged dimer in rHDL which was evident from the product band mobility, as shown in Figure 3A. Therefore, to distinguish between CCL formed between lysines and disulfide cross-links from bridged cysteines present in the starting apoA-I_{Milano}, each cross-linked sample was reduced with β-mercaptoethanol (βME) before SDS−PAGE, as shown in Figure 3B. Since DSP is the only "reducible" cross-linker used, >90% of dimeric bands in lane 2 were lost. However, lanes 3 and 4 showed that after reduction with βME cross-linked products from treatment with BS^3 and EGS still remained. A pictorial representation of these data is shown in Figure 3C.

Cross-linked protein from 125 Å diameter POPC rHDL particles carrying dimeric apoA-I_{Milano} was separated by 4−30% nonreducing gradient SDS−PAGE as shown in Figure 4A or under reducing conditions as shown in Figure 4B. Each gel shows the product distribution following treatment with DSG, lanes 2; DSP, lanes 3; BS^3, lanes 4; EGS, lanes 5; and rHDL containing apoA-I_{Milano}, lanes 6. Figure 4A shows that cross-linking with DSG, DSP, BS^3, and EGS gives protein migrating at a molecular weight consistent with a tetramer composed of four molecules of apoA-I_{Milano}. Analysis of 125 Å diameter rHDL

Table 3: Relative Intensities of Cross-Linked Peptides

sequenced m/z	cross-linker	ID	lysine no.[a]	M[b]	D[b,c]	T[b]
		78 Å Diameter rHDL				
836.96	BS^3	T_{11-13}	88−94	0.2	0.1	
942.84	BS^3	$T_{1\alpha}/T_{2-3}$	1−12	0.1	0.3	
913.14	BS^3	T_{5-6}/T_{35-36}	40−239	0.1	0.7	
872.80	BS^3	T_{6-8}	45−59	0.1	0.2	
783.08	BS^3	T_{31-32}	206−208	0.8	0.8	
820.10	BS^3	T_{13-14}/T_{17-18}	96−118	0.0	0.2	
760.89	BS^3	T_{13-14}/T_{13-14}	96−96	0.0	0.4	
793.66	BS^3	T_{7-8}/T_{20-21}	59−133	0.0	0.5	
768.42	BS^3	T_{20-22}	133−140	1.0	1.0	
777.76	S−S	T_{26-27}/T_{26-27}	173−173	P	P	
		125 Å Diameter rHDL				
836.91	BS^3	T_{11-13}	88−94	1.3	1.0	0.9
731.39	BS^3	T_{13-14}/T_{35-36}	96−239	0.0	0.5	1.3
718.02	BS^3	T_{15-16}/T_{35-36}	107−239	0.0	0.6	3.3
1152.04	BS^3	T_{20-22}	133−140	1.0	1.0	1.0
820.10	BS^3	T_{13-14}/T_{17-18}	96−118	0.0	0.0	0.4
913.14	BS^3	T_{5-6}/T_{35-36}	40−239	0.3	2.4	1.3
1066.04	$BS(PEG)_5$	$T_{1\alpha}/T_{35-36}$	1α-239	0.0	0.0	0.4
799.72	$BS(PEG)_5$	$T_{1\alpha}/T_{17-18}$	1α-118	0.1	0.4	1.6
970.14	$BS(PEG)_5$	$T_{1\alpha}/T_{14-15}$	1α-106	0.1	0.3	0.3
822.77	$BS(PEG)_5$	T_{20-22}	133−140	1.0	1.0	1.0
812.41	EGS	T_{31-32}	206−208	1.5	1.7	1.0
1052.56	EGS	T_{2-4}	12−23	2.1	2.8	1.4
797.74	EGS	T_{20-22}	133−140	1.0	1.0	1.0
777.76	S−S	T_{26-27}/T_{26-27}	173−173	P	P	P

[a]The numbers indicate the lysines that were bridged by the cross-linker. [b]Within a single analysis for monomer (M), dimer (D), or tetramer (T) for each cross-linker, the ion current for each m/z was divided by the ion current for the ubiquitous T_{20-22} intramolecular cross-linked peptide. [c]D represents the sum of the intensity for the two dimer bands, D1 and D2, that has been previously discussed (*25*).

using reductive SDS−PAGE yielded mostly monomer; however, Figure 4B shows that nonreducible dimers were present in preparations cross-linked by BS^3 and EGS and both dimers and trimers present after treatment with DSG. Figure 4C illustrates how chemical cross-linking could yield a tetramer and a dimer and how reduction of these species yields trimeric and dimeric apoA-I_{Milano}. Overall, Figures 3C and 4C suggest that some dimers from 125 Å diameter rHDL might be formed from different lysine−lysine intermolecular cross-links compared to those formed on 78 Å diameter rHDL.

Identification of Lysine−Lysine Cross-Links from ApoA-I_{Milano}. Cross-linked samples were separated under reducing conditions using 4−30% SDS−PAGE. The protein bands were excised and digested with trypsin (*23*, *25*). The extracted peptides were analyzed by ES-MS/MS. After mass correction a peptide list was generated from the survey scan and compared to a theoretical list of all possible peptide intermolecular and intramolecular cross-links for each CCL. After mass correction candidate peptides were assessed by assuming the masses of the experimental and theoretical cross-links were within ±20 ppm. Candidate peptides identified from the survey scans were sequenced by MS/MS. In these experiments the difference between theoretical and experimental values for each cross-linked peptide was ≤8 ppm.

Table 1 shows all of the cross-links identified from 78 Å diameter POPC rHDL using DSP and BS^3 while Table 2 shows all of the cross-links identified from 125 Å diameter POPC rHDL using BS^3, DSG, EGS, and $BS(PEG)_5$. As an internal control, unreduced cross-linked samples were also analyzed. The disulfide cross-link between the two Cys_{173} was detected and sequenced and is listed as T_{26-27}/T_{26-27}, where T indicates that the peptide derived from tryptic cleavage and the subscript refers to the individual tryptic peptides that make up the connected parts. To help ascertain whether the cross-links were intramolecular or intermolecular, the single scan intensity at the m/z of the sequenced monoisotopic ion was extracted from each total ion chromatogram and divided by the intensity of the ubiquitous intramolecular cross-link, T_{20-22} (lysines 133−140), that has been identified using most CCLs. This calculation was performed for each type of CCL used in these studies. Because DSP has a disulfide bridge (Figure 2) that would be reduced under the reducing conditions of the analysis, it was not used for this analysis. The results for both 78 and 125 Å diameter rHDL are summarized in Table 3. After disulfide reduction two protein species were obtained from 78 Å diameter rHDL and three from 125 Å diameter rHDL: M, monomeric apoA-I_{Milano}, D, dimeric apoA-I_{Milano}, and T, tetrameric apoA-I_{Milano}. As discussed in our previous publications (*23*, *25*) CCL yielded two dimers that were combined as a single entity to simplify analysis in Table 3.

Sometimes the sites of cross-linking in peptides, like T_{11-13} where lysines 88 and 94 are connected, suggest that they are intramolecular cross-links in regions that would be suspected of having α-helical character with the lysines located on the same face of the peptide. These peptides have been characterized as intrapeptide cross-links (*54*). Others of this group are T_{2-4}, T_{6-8}, and T_{20-22}. The cross-linked peptide T_{31-32} has lysines adjacent to one another at positions 206 and 208 that do not span a region of α-helix. Other cross-links may arise from intramolecular cross-links between lysines that are close together in space but not near one another in the primary sequence or from intermolecular cross-links between the two protein strands. As an example, compare T_{α}/T_{2-3} and T_{7-8}/T_{20-21} from 78 Å diameter rHDL. In support, Table 3 shows that $T_{1\alpha}/T_{2-3}$ was present in all protein bands; i.e., it is distributed in both monomer and dimer bands like the intrapeptide cross-link T_{20-22}. T_{7-8}/T_{20-21} was detected only in dimer bands, D (Table 3), suggesting that it is an intermolecular CCL. An unusual case was T_{5-6}/T_{35-36} which has a small presence in the monomer, M, but much larger contribution in D from 78 Å diameter rHDL and D and tetramer, T, from 125 Å diameter rHDL. These observations suggest that the conformation of apoA-I_{Milano} puts lysines 40 and 239 close together, giving both intra- and intermolecular association, one product associated with apoA-I_{Milano} monomer and the other with apoA-I_{Milano} dimer.

Molecular Models for ApoA-I_{Milano} Folding. The apoA-I primary and secondary structure was constructed from coordinates for lipid-free Δ43-apoA-I (*34*) joined with 1−43 amino acids, initially as an α-helical segment, and with arginine at position 173 replaced with a cysteine. The two molecules were oriented to accommodate the disulfide cross-link between cysteines at position 173 on each protein. Then the chemical cross-links were oriented to the correct distances based on whether these cross-links were intramolecular or intermolecular. We used the maximum distance of C_{α}-lysine−(cross-linker)−C_{α}-lysine calculated for each of the cross-linkers to establish the appropriate separation. To accommodate the cross-links, apoA-I was bent only at the proline or glycine−glycine sites between the amphipathic segments of apoA-I. Of particular interest are the sequenced cross-links T_{5-6}/T_{35-36} (lysines 40 and 239), shown in Figure 5A, that span one end of the molecule to the other and

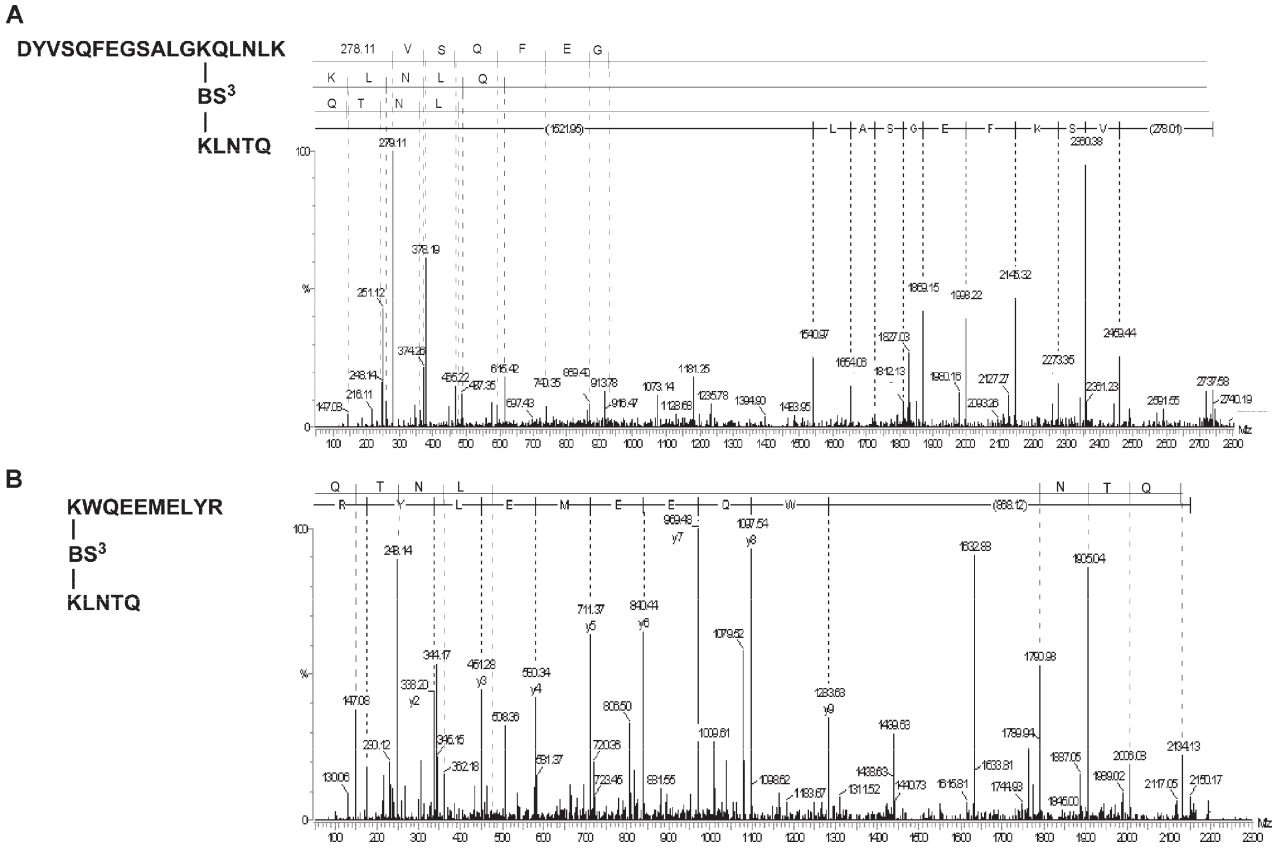

FIGURE 5: Verification of the Q-TOF-MS/MS spectrum. Panel A shows the Q-TOF-MS/MS spectrum of the T_{5-6}/T_{35-36} (lysines 40−239) cross-linked peptide from 78 Å diameter rHDL treated with BS^3. The MS/MS spectrum was obtained from the triply charged ion having $m/z = 913.14$ that gives a singly protonated mass of 2737.4348 Da. Panel B shows the Q-TOF-MS/MS spectrum of T_{15-16}/T_{35-36} (lysines 107−239) cross-linked peptide from 125 Å diameter rHDL treated with BS^3. The MS/MS spectrum was obtained from the triply charged ion having $m/z = 718.02$ and a singly protonated mass of 2152.0525 Da. The sequences are shown using single letter abbreviations for the amino acids. y-Series start with either K or R. Details are reported in the section on Experimental Procedures.

suggest N- and C-termini are proximate. Other cross-links like T_{15-16}/T_{35-36} (lysines 107 and 235), shown in Figure 5B, along with the intermolecular cross-link between amino acids 173 define the antiparallel orientation of the two apoA-I_{Milano} chains. One assumption that we made was that the cross-links represented only a single conformation.

DISCUSSION

To construct a three-dimensional model of apoA-I_{Milano}, we assumed that the conformation of the central region of the dimer would be similar to apoA-I_{WT} monomers on 80 and 96 Å diameter rHDL. Using these assumptions and the chemical cross-links as physical constraints, we obtained a particle with an outer diameter of about 78 Å and an internal diameter of about 57 Å. Using the POPC bilayer area of 68.3 $Å^2$ (*55*) this internal region would hold about 37 POPC per particle face for a total of 74 POPC per particle. Experimental measurement shows there are 76 POPC per particle. If the "belt buckle" conformation proposed for apoA-I_{WT} (*25*) is used as a preliminary model, the frame shift induced by the cysteine-173 to cysteine-73 disulfide cross-link leaves part of the hydrophobic region on the edge of the particle exposed to aqueous solvent. We speculate that, to compensate, the C-terminal end covers the hydrophobic edge of the particle putting the C-terminal and N-terminal ends close to one another as shown by the lysine-40 to lysine-239 cross-link. This change in the C-terminal conformation may explain why the 78 Å apoA-I_{WT} rHDL is apparently a less stable particle as suggested by the large signature on separation by nonreducing gradient gel electrophoresis (Figure 1). We propose that the N-terminal ends of dimeric apoA-I_{Milano} fold back similar to that reported for 80 Å apoA-I_{WT} rHDL (*25*).

The BS^3 intermolecular cross-links between lysines-96 and between lysine-59 and lysine-133 on each apoA-I_{Milano} strongly suggest an antiparallel alignment for the two strands. If the conformation is an antiparallel "belt-like loop", similar to that suggested for 80 Å diameter apoA-I_{WT} (*25*), then lysines at position 96 on each strand would be close to one another. Furthermore, an intramolecular cross-link between lysines-40 and lysine-239 suggests that the N-terminal regions are close to their respective C-terminus. After connecting the cross-links listed above, lysines 40 and 239 on the opposite strands were next to one another. In Table 3 the reduced, digested peptides from CCL apoA-I dimers, that run at about 55 kDa, show a large amount of the lysine 40−lysine-239 cross-link compared to the digested peptides from apoA-I_{Milano} that runs as a monomer at 28 kDa, consistent with the hypothesis that the N-terminal end of one apoA-I molecule is close to the C-terminal end of the second molecule and that they can be coupled to give an intermolecular cross-link.

Figure 6 shows the conformation we propose for the orientation of a single apoA-I_{Milano} dimer bound to a 78 Å diameter rHDL. The "belt" conformation of apoA-I_{Milano} on the rHDL model is saddle-shaped like the starting coordinates used for the model and similar to the conformation that was reported after modeling phospholipid and modified forms of apoA-I_{WT} that was missing either the first 40 amino acids (*56*) or the first

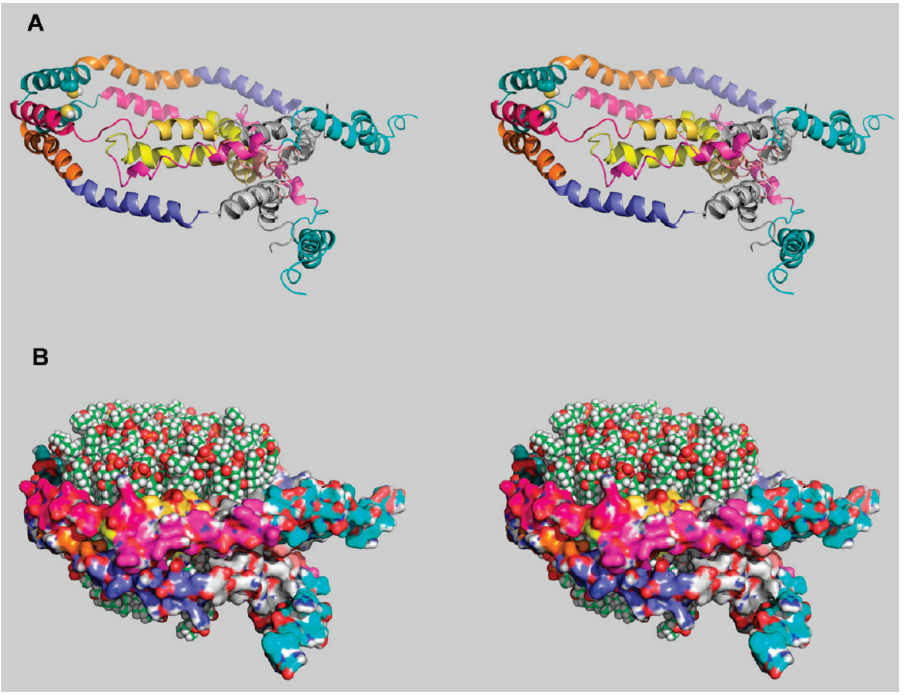

FIGURE 6: Conformation for dimeric apoA-I_{Milano} on a 78 Å diameter POPC rHDL particle. Panels A and B show the three-dimensional conformation for 1 dimer of apoA-I_{Milano} bound to a 78 Å diameter POPC rHDL particle. MS/MS sequenced cross-links (Table 1) were used as molecular constraints for modeling the lipid-bound conformation of dimeric apoA-I_{Milano} on 78 Å particles. Panel A shows dimeric apoA-I_{Milano} is locked by a single cysteine−cysteine disulfide bond at position 173 on each monomer. Although the structure resembles the antiparallel "belt-like" conformation reported for 80 Å apoA-I_{WT} on POPC rHDL (*25*), the C-terminal end of each monomer does not fold back on itself as it does for apoA-I_{WT}, but instead the C-terminal end wraps around the periphery. Each helical region is shown in a different color. Panel B shows the bilayer contains 76 molecules of POPC, and the model was generated using the membrane plugin, version 1.1, by I. Balabin available in VMD version 1.8.7 (*53*). Protein is shown as a surface for simplicity.

11 to 22 amino acids (*57*). The effect of the disulfide cross-link is apparent by comparing these results to those obtained from particles prepared with monomeric apoA-I_{Milano}. Our preliminary results using CCL/MS of monomeric apoA-I_{Milano} rHDL support a "belt" model (data not shown) identical to that reported for apoA-I_{WT} (*23*, *25*) and calculated for apoA-I_{Milano} (*22*).

In contrast to a "belt" of protein wrapped around a bilayer of lipid, Wu et al. (*28*) suggested a "double super helix" model for the conformation of apoA-I_{WT} on 96 Å diameter rHDL composed of POPC, cholesterol, and apoA-I_{WT} in a ratio of 89:10:1. The relationship between the two monomer strands is antiparallel with the helix 5 to helix 5 regions, amino acids 121−142, adjacent one to another. The protein conformation can be described as having an open helical shape reminiscent of the shapes derived from computational methods with low phospholipid to apoA-I ratios (*56*). For apoA-I_{Milano} the intramolecular cross-link between lysine-40 and lysine-239 shows that the N- and C-terminal regions of a single apoA-I strand are close together and, therefore, apoA-I_{Milano} may not preferentially adopt a "double super helix" conformation. Silva et al. (*26*) have proposed that there are two possible registries for the apoA-I monomers: the first is the helix 5 to helix 5 discussed above and the second is a helix 5 to helix 2 registry. The disulfide bond fixes a helix 7 to helix 7 registry that does not allow overlap between helix 5 and helix 2. These data strongly suggest a conformational restriction imposed by the helix 7 to helix 7 cysteine linkage present in the apoA-I_{Milano} dimer, which may lead to a significant change in the ability of the apoprotein to stably accommodate phospholipids particularly evident by the diffuse banding seen for the 78 Å rHDL containing apoA-I_{Milano} dimer (Figure 1, lane 1).

There are two differences in the cross-link pattern for large diameter particles compared to the pattern for the 78 Å diameter particles. Two BS^3 cross-links present in the 78 Å particles, lysine-96 to lysine-96 and lysine-59 to lysine-133 were not present in the 125 Å diameter rHDL, while two new BS^3 cross-links appear in the larger particles, connections between lysine-96 and lysine-239 and between lysine-107 and lysine-239. Three cross-links from $BS(PEG)_5$ were identified for the 125 Å diameter particles. Of these cross-links, Table 3 suggests that 1α-239 was exclusively an intermolecular cross-link and 1α-106 was exclusively an intramolecular cross-link, while 1α-118 has both intermolecular and intramolecular components. That the 1α position has yielded so many cross-links suggests that it may have conformation freedom not available to the other positions in the molecule.

Our first hypothesis was that the protein strands encircling 125 Å diameter rHDL had a greater diameter compared to 78 Å diameter rHDL. Three sets of cross-links, the intermolecular disulfide link 173 to 173, the intramolecular and intermolecular lysine-40 to lysine-239, the intermolecular lysine-96 to lysine-239 and lysine-107 to lysine-239 suggested that the diameter of dimeric apoA-I_{Milano} in 125 Å diameter rHDL was closer to the diameter of the 96 Å diameter rHDL. From Tables 2 and 3 we assume that cross-links lysine-96 to lysine-118 and aspartic acid-1α to lysine-239 were involved in tying together the two dimers. We speculate that two dimeric apoA-I_{Milano} molecules were stacked adjacent one another oriented such that lysine-96 on one of the apoA-I_{Milano} dimer strands was close to lysine-118 of the second dimer. Figure 7 shows our proposed conformation for two dimers of apoA-I_{Milano} bound to a 125 Å diameter rHDL. For the model shown in Figure 7 the maximum atom to atom diagonal distance from the top strand to the bottom strand was about 96 Å.

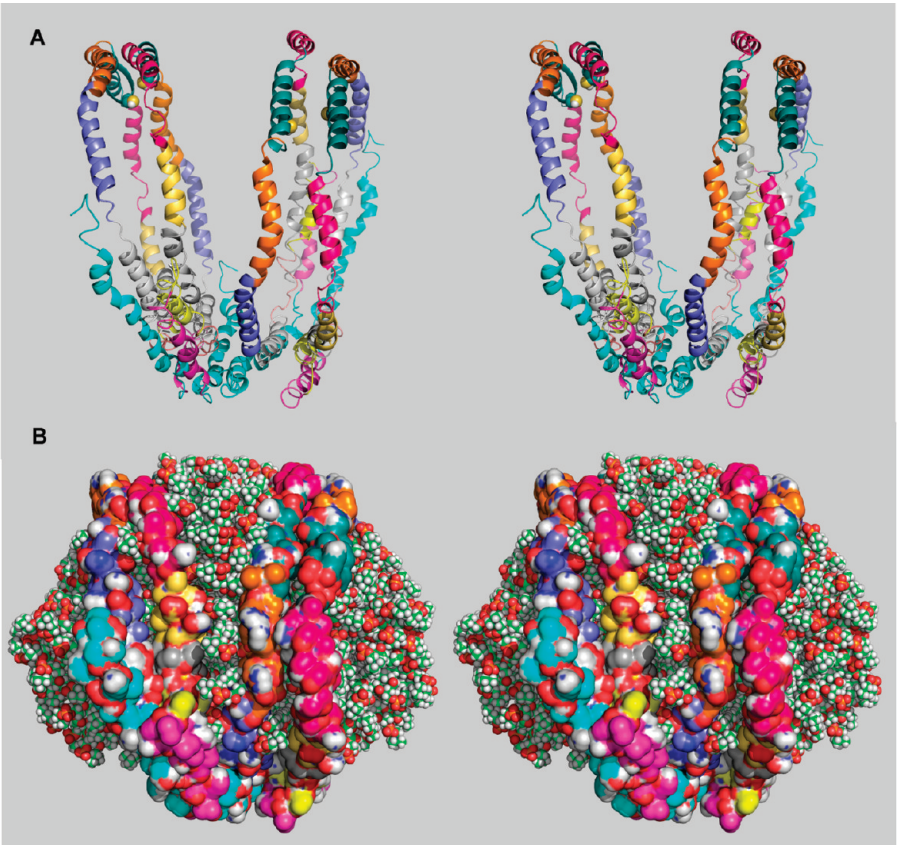

FIGURE 7: Conformation for a 125 Å diameter POPC rHDL particle containing two dimers of apoA-I_{Milano}. Panels A and B show the three-dimensional conformation for two molecules of dimeric apoA-I_{Milano} bound to a 125 Å diameter POPC rHDL particle. MS/MS sequenced cross-links (Table 2) were used as molecular constraints for modeling the lipid-bound conformation of dimeric apoA-I_{Milano}. In panel A, each of the two dimeric apoA-I_{Milano} is locked by a single cysteine−cysteine disulfide bond at position 173. Each helical region is shown in a different color. Panel B shows the bilayer contains 209 molecules of POPC, and the model was generated using the membrane plugin, version 1.1, by I. Balabin available in VMD version 1.8.7 (*53*). For simplicity protein is shown as a surface.

The orientation of the lipid poses a curious conundrum for the 125 Å diameter rHDL. In the smaller particles apoA-I_{Milano} is envisioned to enclose the bilayer associating with the nonpolar edge of the POPC bilayer. We address the question of lipid packing by first noting the depth of a POPC membrane bilayer is roughly 36 Å. For a single pair of apoA-I molecules computational studies suggest that POPC hydrophobic regions associate with the hydrophobic region of the amphipathic helix (*22*, *28*, *39*, *41*, *56*). Previous studies of the binding of amphipathic α-helical peptides 2F and 4F to DOPC multilayers (*58*) indicated that these peptides bury themselves so that the center of the α-helix is located about 17.1 Å from the hydrophobic face, about the level of the glycerol backbone, 17.6 Å (*59*). High-resolution NMR analyses of the DMPC/2F and DMPC/4F complexes suggested that the α-helical peptide was aligned perpendicular to the acyl chains (*60*, *61*). If the apoA-I protein strands align themselves perpendicular to the fatty acyl chains of POPC, our "belt" model for the 78 Å diameter POPC/apoA-I_{Milano} complex is consistent with our cross-linking results. However, a flat bilayer structure does not seem to be well suited for representing the larger diameter particle. To obtain a structure having the hydrophobic region of the amphipathic α-helices interacting with the fatty acyl chains suggests that POPC behaves like a laminar micelle (*62*) and that the POPC/apoA-I_{Milano} complex assumes an ellipsoidal shape.

Several studies have suggested less effective LCAT-catalyzed remodeling of small apoA-I_{Milano}-containing particles compared to the remodeling of apoA-I_{WT}-containing rHDL (*63*−*65*). The regions of apoA-I that have been associated with LCAT binding (*47*, *66*−*73*), most of helix 6 (amino acids 143−164), were located closer together in the models for both apoA-I_{Milano}-containing particles compared to the same regions in apoA-I_{WT}-containing disks (*25*, *73*). This conformational change may well affect the binding of LCAT to rHDL (*64*, *65*, *74*).

In conclusion, we report low-resolution three-dimensional conformations for dimeric apoA-I_{Milano} bound to POPC rHDLs. The results suggest that the overall protein conformation is a "belt," similar to the conformation proposed for apoA-I_{WT}. In addition, both apoA-I_{Milano} and apoA-I_{WT} appear to have an N-terminal region that spends a finite amount of time folded back over the "belt" or central region of the protein. The feature unique to apoA-I_{Milano} compared to apoA-I_{WT} is that for apoA-I_{Milano} the C-termini appear to wrap around the periphery of the particle. Functionally, these models suggest that the regions associated with LCAT activity (helices 5−7) have been pushed together and thus possibly reducing exposure of the region which is usually accessible to LCAT and thus vital for activation of the enzyme.

ACKNOWLEDGMENT

The Waters Q-TOF mass spectrometer was purchased with funds from NIH Shared Instrumentation Grant 1S10RR17846 (M.J.T.). The MS analyses were performed in the Mass Spectrometer Facility of the Comprehensive Cancer Center of Wake Forest University School of Medicine, supported in part by NCI center grant 5P30CA12197.

REFERENCES

1. Yancey, P. G., Bortnick, A. E., Kellner-Weibel, G., De La Llera-Moya, M., Phillips, M. C., and Rothblat, G. H. (2003) Importance of different pathways of cellular cholesterol efflux. *Arterioscler., Thromb. Vasc. Biol. 23*, 712–719.
2. Libby, P. (2001) Managing the risk of atherosclerosis: The role of high-density lipoprotein. *Am. J. Cardiol. 88*, 3N–8N.
3. Kwiterovich, P. O. (1998) The antiatherogenic role of high-density lipoprotein cholesterol. *Am. J. Cardiol. 82*, 13Q–21Q.
4. Boden, W. E. (2000) High-density lipoprotein cholesterol as an independent risk factor in cardiovascular disease: Assessing the data from Framingham to the Veterans Affairs high-density lipoprotein intervention trial. *Am. J. Cardiol. 86*, 19L–22L.
5. Harper, C. R., and Jacobson, T. A. (1999) New perspectives on the management of low levels of high-density lipoprotein cholesterol. *Arch. Intern. Med. 159*, 1049–1057.
6. Libby, P. (2001) What have we learned about the biology of atherosclerosis? The role of inflammation. *Am. J. Cardiol. 88*, 3J–6J.
7. Gualandri, V., Orsini, G. B., Cerrone, A., Franceschini, G., and Sirtori, C. R. (1985) Familial associations of lipids and lipoproteins in a highly consanguineous population: The Limone sul Garda study. *Metabolism 34*, 212–221.
8. Sirtori, C. R., Calabresi, L., Franceschini, G., Baldassarre, D., Amato, M., Johansson, J., Salvetti, M., Monteduro, C., Zulli, R., Muiesan, M. L., and Agabiti-Rosei, E. (2001) Cardiovascular status of carriers of the apolipoprotein A-I(Milano) mutant: the Limone sul Garda study. *Circulation 103*, 1949–1954.
9. Nissen, S. E., Tsunoda, T., Tuzcu, E. M., Schoenhagen, P., Cooper, C. J., Yasin, M., Eaton, G. M., Lauer, M. A., Sheldon, W. S., Grines, C. L., Halpern, S., Crowe, T., Blankenship, J. C., and Kerensky, R. (2003) Effect of recombinant ApoA-I Milano on coronary atherosclerosis in patients with acute coronary syndromes: A randomized controlled trial. *J. Am. Med. Assoc. 290*, 2292–2300.
10. Tardif, J. C., Gregoire, J., L'Allier, P. L., Ibrahim, R., Lesperance, J., Heinonen, T. M., Kouz, S., Berry, C., Basser, R., Lavoie, M. A., Guertin, M. C., and Rodes-Cabau, J. (2007) Effects of reconstituted high-density lipoprotein infusions on coronary atherosclerosis: a randomized controlled trial. *J. Am. Med. Assoc. 297*, 1675–1682.
11. Shah, P. K., Nilsson, J., Kaul, S., Fishbein, M. C., Ageland, H., Hamsten, A., Johansson, J., Karpe, F., and Cercek, B. (1998) Effects of recombinant apolipoprotein A-I_{Milano} on aortic atherosclerosis in apolipoprotein E-deficient mice. *Circulation 97*, 780–785.
12. Shah, P. K., Kaul, S., Nilsson, J., and Cercek, B. (2001) Exploiting the vascular protective effects of high-density lipoprotein and its apolipoproteins: An idea whose time for testing is coming, part II. *Circulation 104*, 2498–2502.
13. Shah, P. K., Kaul, S., Nilsson, J., and Cercek, B. (2001) Exploiting the vascular protective effects of high-density lipoprotein and its apolipoproteins: An idea whose time for testing is coming, part I. *Circulation 104*, 2376–2383.
14. Wang, L., Sharifi, B. G., Pan, T., Song, L., Yukht, A., and Shah, P. K. (2006) Bone marrow transplantation shows superior atheroprotective effects of gene therapy with apolipoprotein A-I Milano compared with wild-type apolipoprotein A-I in hyperlipidemic mice. *J. Am. Coll. Cardiol. 48*, 1459–1468.
15. Chiesa, G., Monteggia, E., Marchesi, M., Lorenzon, P., Laucello, M., Lorusso, V., Di Mario, C., Karvouni, E., Newton, R. S., Bisgaier, C. L., Franceschini, G., and Sirtori, C. R. (2002) Recombinant apolipoprotein A-I(Milano) infusion into rabbit carotid artery rapidly removes lipid from fatty streaks. *Circ. Res. 90*, 974–980.
16. Marchesi, M., Booth, E. A., Davis, T., Bisgaier, C. L., and Lucchesi, B. R. (2004) Apolipoprotein A-IMilano and 1-palmitoyl-2-oleoyl phosphatidylcholine complex (ETC-216) protects the in vivo rabbit heart from regional ischemia-reperfusion injury. *J. Pharmacol. Exp. Ther. 311*, 1023–1031.
17. Marchesi, M., Booth, E. A., Rossoni, G., Garcia, R. A., Hill, K. R., Sirtori, C. R., Bisgaier, C. L., and Lucchesi, B. R. (2008) Apolipoprotein A-IMilano/POPC complex attenuates post-ischemic ventricular dysfunction in the isolated rabbit heart. *Atherosclerosis 197*, 572–578.
18. Kaul, S., Rukshin, V., Santos, R., Azarbal, B., Bisgaier, C. L., Johansson, J., Tsang, V. T., Chyu, K. Y., Cercek, B., Mirocha, J., and Shah, P. K. (2003) Intramural delivery of recombinant apolipoprotein A-IMilano/phospholipid complex (ETC-216) inhibits in-stent stenosis in porcine coronary arteries.
19. Parolini, C., Chiesa, G., Zhu, Y., Forte, T., Caligari, S., Gianazza, E., Sacco, M. G., Sirtori, C. R., and Rubin, E. M. (2003) Targeted replacement of mouse apolipoprotein A-I with human ApoA-I or the mutant ApoA-IMilano. Evidence of APOA-IM impaired hepatic secretion. *J. Biol. Chem. 278*, 4740–4746.
20. Parolini, C., Chiesa, G., Gong, E., Caligari, S., Cortese, M. M., Koga, T., Forte, T. M., and Rubin, E. M. (2005) Apolipoprotein A-I and the molecular variant apoA-I(Milano): Evaluation of the antiatherogenic effects in knock-in mouse model. *Atherosclerosis 183*, 222–229.
21. Lebherz, C., Sanmiguel, J., Wilson, J. M., and Rader, D. J. (2007) Gene transfer of wild-type apoA-I and apoA-I Milano reduce atherosclerosis to a similar extent. *Cardiovasc. Diabetol. 6*, 6–15.
22. Klon, A. E., Jones, M. K., Segrest, J. P., and Harvey, S. C. (2000) Molecular belt models for the apolipoprotein A-I Paris and Milano mutations. *Biophys. J. 79*, 1679–1685.
23. Bhat, S., Sorci-Thomas, M. G., Alexander, E. T., Samuel, M. P., and Thomas, M. J. (2005) Intermolecular contact between globular N-terminal fold and C-terminal domain of ApoA-I stabilizes its lipid-bound conformation: studies employing chemical cross-linking and mass spectrometry. *J. Biol. Chem. 280*, 33015–33025.
24. Calabresi, L., Vecchio, G., Longhi, R., Gianazza, E., Palm, G., Wadensten, H., Hammarstrom, A., Olsson, A., Karlstrom, A., and Sejlitz, T.; et al. (1994) Molecular characterization of native and recombinant apolipoprotein A-IMilano dimer. The introduction of an interchain disulfide bridge remarkably alters the physicochemical properties of apolipoprotein A-I. *J. Biol. Chem. 269*, 32168–32174.
25. Bhat, S., Sorci-Thomas, M. G., Tuladhar, R., Samuel, M. P., and Thomas, M. J. (2007) Conformational adaptation of apolipoprotein A-I to discretely sized phospholipid complexes. *Biochemistry 46*, 7811–7821.
26. Silva, R. A., Hilliard, G. M., Li, L., Segrest, J. P., and Davidson, W. S. (2005) A mass spectrometric determination of the conformation of dimeric apolipoprotein A-I in discoidal high density lipoproteins. *Biochemistry 44*, 8600–8607.
27. Davidson, W. S., and Hilliard, G. M. (2003) The spatial organization of apolipoprotein A-I on the edge of discoidal high density lipoprotein particles—A mass spectrometry study. *J. Biol. Chem. 278*, 27199–27207.
28. Wu, Z., Gogonea, V., Lee, X., Wagner, M. A., Li, X. M., Huang, Y., Undurti, A., May, R. P., Haertlein, M., Moulin, M., Gutsche, I., Zaccai, G., Didonato, J. A., and Hazen, S. L. (2009) The double super helix model of high density lipoprotein, J. Biol. Chem.
29. Wu, Z., Wagner, M. A., Zheng, L., Parks, J. S., Shy, J. M., III, Smith, J. D., Gogonea, V., and Hazen, S. L. (2007) The refined structure of nascent HDL reveals a key functional domain for particle maturation and dysfunction, Nat. Struct. Mol. Biol. *14*, 861−868 [erratum: *Nat. Struct. Mol. Biol.* (2008) 2015, 2330].
30. Panagotopulos, S. E., Horace, E. M., Maiorano, J. N., and Davidson, W. S. (2001) Apolipoprotein A-I adopts a belt-like orientation in reconstituted high density lipoproteins. *J. Biol. Chem. 276*, 42965–42970.
31. Maiorano, J. N., Jandacek, R. J., Horace, E. M., and Davidson, W. S. (2004) Identification and structural ramifications of a hinge domain in apolipoprotein A-I discoidal high-density lipoproteins of different size. *Biochemistry 43*, 11717–11726.
32. Li, H., Lyles, D. S., Thomas, M. J., Pan, W., and Sorci-Thomas, M. G. (2000) Structural determination of lipid-bound ApoA-I using fluorescence resonance energy transfer. *J. Biol. Chem. 275*, 37048–37054.
33. Li, H. H., Thomas, M. J., Pan, W., Alexander, E., Samuel, M., and Sorci-Thomas, M. G. (2001) Preparation and incorporation of probe-labeled apoA-I for fluorescence resonance energy transfer studies of rHDL. *J. Lipid Res. 42*, 2084–2091.
34. Borhani, D. W., Rogers, D. P., Engler, J. A., and Brouillette, C. G. (1997) Crystal structure of truncated human apolipoprotein A-I suggests a lipid-bound conformation. *Proc. Natl. Acad. Sci. U.S.A. 94*, 12291–12296.
35. Tricerri, M. A., Behling Agree, A. K., Sanchez, S. A., Bronski, J., and Jonas, A. (2001) Arrangement of apolipoprotein A-I in reconstituted high-density lipoprotein disks: An alternative model based on fluorescence resonance energy transfer experiments. *Biochemistry 40*, 5065–5074.
36. Segrest, J. P., Jones, M. K., Klon, A. E., Sheldahl, C. J., Hellinger, M., De Loof, H., and Harvey, S. C. (1999) A detailed molecular belt model for apolipoprotein A-I in discoidal high density lipoprotein. *J. Biol. Chem. 274*, 31755–31758.
37. Klon, A. E., Segrest, J. P., and Harvey, S. C. (2002) Comparative models for human apolipoprotein A-I bound to lipid in discoidal high-density lipoprotein particles. *Biochemistry 41*, 10895–10905.
38. Klon, A. E., Segrest, J. P., and Harvey, S. C. (2002) Molecular dynamics simulations on discoidal HDL particles suggest a mechanism for rotation in the apo A-I belt model. *J. Mol. Biol. 324*, 703–721.

39. Rocco, A. G., Gianazza, E., Calabresi, L., Sensi, C., Franceschini, G., Sirtori, C. R., and Eberini, I. (2009) Structural features and dynamics properties of human apolipoprotein A-I in a model of synthetic HDL. *J. Mol. Graphics Modell. 28*, 305–312.
40. Shih, A. Y., Sligar, S. G., and Schulten, K. (2008) Molecular models need to be tested: The case of a solar flares discoidal HDL model. *Biophys. J. 94*, L87–L89.
41. Shih, A. Y., Arkhipov, A., Freddolino, P. L., Sligar, S. G., and Schulten, K. (2007) Assembly of lipids and proteins into lipoprotein particles. *J. Phys. Chem. B 111*, 11095–11104.
42. Li, H. H., Lyles, D. S., Pan, W., Alexander, E., Thomas, M. J., and Sorci-Thomas, M. G. (2002) ApoA-I structure on discs and spheres. Variable helix registry and conformational states. *J. Biol. Chem. 277*, 39093–39101.
43. Martin, D. D., Budamagunta, M. S., Ryan, R. O., Voss, J. C., and Oda, M. N. (2006) Apolipoprotein A-I assumes a "looped belt" conformation on reconstituted high density lipoprotein. *J. Biol. Chem. 281*, 20418–20426.
44. Calabresi, L., Vecchio, G., Frigerio, F., Vavassori, L., Sirtori, C. R., and Franceschini, G. (1997) Reconstituted high-density lipoproteins with a disulfide-linked apolipoprotein A-I dimer: Evidence for restricted particle size heterogeneity. *Biochemistry 36*, 12428–12433.
45. Jonas, A. (1987) Lecithin cholesterol acyltransferase, in Plasma Lipoproteins (Gotto, A. M., Jr., Ed.) pp 299−333, Elsevier, Amsterdam.
46. Sorci-Thomas, M. G., Parks, J. S., Kearns, M. W., Pate, G. N., Zhang, C., and Thomas, M. J. (1996) High level secretion of wild-type and mutant forms of human proapoA-I using baculovirus-mediated Sf-9 cell expression. *J. Lipid Res. 37*, 673–683.
47. Alexander, E. T., Bhat, S., Thomas, M. J., Weinberg, R. B., Cook, V. R., Bharadwaj, M. S., and Sorci-Thomas, M. (2005) Apolipoprotein A-I helix 6 negatively charged residues attenuate lecithin-cholesterol acyltransferase (LCAT) reactivity. *Biochemistry 44*, 5409–5419.
48. Lagerstedt, J. O., Budamagunta, M. S., Oda, M. N., and Voss, J. C. (2007) EPR spectroscopy of site-directed spin labels reveals the structural heterogeneity in the N-terminal domain of apo-AI in solution. *J. Biol. Chem. 282*, 9143–9149.
49. Zhu, H. L., and Atkinson, D. (2004) Conformation and lipid binding of the N-terminal (1−44) domain of human apolipoprotein A-I. *Biochemistry 43*, 13156–13164.
50. Okon, M., Frank, P. G., Marcel, Y. L., and Cushley, R. J. (2002) Heteronuclear NMR studies of human serum apolipoprotein A-I. Part I. Secondary structure in lipid-mimetic solution. *FEBS Lett. 517*, 139–143.
51. Segrest, J. P., Jones, M. K., De Loof, H., Brouillette, C. G., Venkatachalapathi, Y. V., and Anantharamaiah, G. M. (1992) The amphipathic helix in the exchangeable apolipoproteins: A review of secondary structure and function. *J. Lipid Res. 33*, 141–166.
52. Silva, R. A., Hilliard, G. M., Fang, J., Macha, S., and Davidson, W. S. (2005) A three-dimensional molecular model of lipid-free apolipoprotein A-I determined by cross-linking/mass spectrometry and sequence threading. *Biochemistry 44*, 2759–2769.
53. Humphrey, W., Dalke, A., and Schulten, K. (1996) VMD: Visual molecular dynamics. *J. Mol. Graphics 14*, 33–38.
54. Bennett, K. L., Kussmann, M., Björk, P., Godzwon, M., Mikkelsen, M., Sørensen, P., and Roepstorff, P. (2000) Chemical cross-linking with thiol-cleavable reagents combined with differential mass spectrometric peptide mapping—A novel approach to assess intermolecular protein contacts. *Protein Sci. 9*, 1503–1518.
55. Zhang, Z., Bhide, S. Y., and Berkowitz, M. L. (2007) Molecular dynamics simulations of bilayers containing mixtures of sphingomyelin with cholesterol and phosphatidylcholine with cholesterol. *J. Phys. Chem. B 111*, 12888–12897.
56. Catte, A., Patterson, J. C., Jones, M. K., Jerome, W. G., Bashtovyy, D., Su, Z., Gu, F., Chen, J., Aliste, M. P., Harvey, S. C., Li, L., Weinstein, G., and Segrest, J. P. (2006) Novel changes in discoidal high density lipoprotein morphology: A molecular dynamics study. *Biophys. J. 90*, 4345–4360.
57. Shih, A. Y., Denisov, I. G., Phillips, J. C., Sligar, S. G., and Schulten, K. (2005) Molecular dynamics simulations of discoidal bilayers assembled from truncated human lipoproteins. *Biophys. J. 88*, 548–556.
58. Mishra, V. K., Palgunachari, M. N., Segrest, J. P., and Anantharamaiah, G. M. (1994) Interactions of synthetic peptide analogs of the class A amphipathic helix with lipids. Evidence for the snorkel hypothesis. *J. Biol. Chem. 269*, 7185–7191.
59. Hristova, K., Wimley, W. C., Mishra, V. K., Anantharamiah, G. M., Segrest, J. P., and White, S. H. (1999) An amphipathic alpha-helix at a membrane interface: A structural study using a novel X-ray diffraction method. *J. Mol. Biol. 290*, 99–117.
60. Mishra, V. K., Anantharamaiah, G. M., Segrest, J. P., Palgunachari, M. N., Chaddha, M., Sham, S. W., and Krishna, N. R. (2006) Association of a model class A (apolipoprotein) amphipathic alpha helical peptide with lipid: High resolution NMR studies of peptide·lipid discoidal complexes. *J. Biol. Chem. 281*, 6511–6519.
61. Mishra, V. K., Palgunachari, M. N., Krishna, R., Glushka, J., Segrest, J. P., and Anantharamaiah, G. M. (2008) Effect of leucine to phenylalanine substitution on the nonpolar face of a class A amphipathic helical peptide on its interaction with lipid: High resolution solution NMR studies of 4F-dimyristoylphosphatidylcholine discoidal complex. *J. Biol. Chem. 283*, 34393–34402.
62. Peters-Libeu, C. A., Newhouse, Y., Hall, S. C., Witkowska, H. E., and Weisgraber, K. H. (2007) Apolipoprotein E*dipalmitoylphosphatidylcholine particles are ellipsoidal in solution. *J. Lipid Res. 48*, 1035–1044.
63. Calabresi, L., Franceschini, G., Burkybile, A., and Jonas, A. (1997) Activation of lecithin cholesterol acyltransferase by a disulfide-linked apolipoprotein A-I dimer. *Biochem. Biophys. Res. Commun. 232*, 345–349.
64. Bielicki, J. K., Forte, T. M., McCall, M. R., Stoltzfus, L. J., Chiesa, G., Sirtori, C. R., Franceschini, G., and Rubin, E. M. (1997) High density lipoprotein particle size restriction in apolipoprotein A-I-(Milano) transgenic mice. *J. Lipid Res. 38*, 2314–2321.
65. Bielicki, J. K., McCall, M. R., Stoltzfus, L. J., Ravandi, A., Kuksis, A., Rubin, E. M., and Forte, T. M. (1997) Evidence that apolipoprotein A-I_{Milano} has reduced capacity, compared with wild-type apolipoprotein A-I, to recruit membrane cholesterol. *Arterioscler., Thromb. Vasc. Biol. 17*, 1637–1643.
66. Sorci-Thomas, M. G., and Thomas, M. J. (2002) The effects of altered apolipoprotein A-I structure on plasma HDL concentration. *Trends Cardiovasc. Med. 12*, 121–128.
67. Sorci-Thomas, M., Kearns, M. W., and Lee, J. P. (1993) Apolipoprotein A-I domains involved in lecithin-cholesterol acyltransferase activation. Structure:function relationships. *J. Biol. Chem. 268*, 21403–21409.
68. Sorci-Thomas, M. G., Thomas, M., Curtiss, L., and Landrum, M. (2000) Single repeat deletion in apoA-I blocks cholesterol esterification and results in rapid catabolism of D6 and wild-type apoA-I in transgenic mice. *J. Biol. Chem. 275*, 12156–12163.
69. McManus, D. C., Scott, B. R., Franklin, V., Sparks, D. L., and Marcel, Y. L. (2001) Proteolytic degradation and impaired secretion of an apolipoprotein A-I mutant associated with dominantly inherited hypoalphalipoproteinemia. *J. Biol. Chem. 276*, 21292–21302.
70. Roosbeek, S., Vanloo, B., Duverger, N., Caster, H., Breyne, J., De Beun, I., Patel, H., Vandekerckhove, J., Choulders, C., Rosseneu, M., and Peelman, F. (2001) Three arginine residues in apolipoprotein A-I are critical for activation of lecithin:cholesterol acyltransferase. *J. Lipid Res. 42*, 31–40.
71. Maiorano, J. N., Jandacek, R. J., Horace, E. M., and Davidson, W. S. (2004) Identification and structural ramifications of a hinge domain in apolipoprotein A-I discoidal high-density lipoproteins of different size. *Biochemistry 43*, 11717–11726.
72. Sorci-Thomas, M. G., Curtiss, L., Parks, J. S., Thomas, M. J., Kearns, M. W., and Landrum, M. (1998) The hydrophobic face orientation of apolipoprotein A-I amphipathic helix domain 143−164 regulates lecithin:cholesterol acyltransferase activation. *J. Biol. Chem. 273*, 11776–11782.
73. Sorci-Thomas, M. G., Bhat, S., and Thomas, M. J. (2009) Lecithin: cholesterol acyltransferase. *Clin. Lipidol./Future Med. 4*, 113–124.
74. Alexander, E. T., Tanaka, M., Kono, M., Saito, H., Rader, D. J., and Phillips, M. C. (2009) Structural and functional consequences of the milano mutation (R173C) in human apolipoprotein A-I. *J. Lipid Res. 50*, 1409–1419.